Fundamental mechanisms of single-pulse NMR echo formation

L. N. Shakhmuratova, D. K. Fowler, and D. H. Chaplin
School of Physics, University College, UNSW, Australian Defence Force Academy, Canberra, ACT 2600, Australia
(Received 30 September 1996)

A theoretical investigation of the formation of the so-called single pulse NMR echo has been undertaken in the presence of both Larmor and Rabi frequency inhomogeneities. It is found that this echo phenomenon, together with weaker, equally spaced secondary echoes, evolves from multiple-pulse excitation under certain constraints with respect to interpulse time intervals compared with longitudinal and transverse relaxation times. These transient coherences arise from a complex superposition of oscillatory free induction decays, which extend further into the time domain because of cumulative dephasing within each pulse in a multiple-pulse sequence. The effect is present for large Larmor inhomogeneity in isolation, but is stronger in the simultaneous presence of both frequency inhomogeneities, characteristic of ferromagnets. Predictions of this model analysis are confirmed through experiment via conventional, zero-field, pulsed NMR on binary ^{51}V*Fe* and pure elementary (enriched) ^{57}Fe*Fe* ferromagnets. [S1050-2947(97)08803-3]

PACS number(s): 33.25.+k, 33.40.+f

I. INTRODUCTION

The single pulse (SP), one pulse, or ''edge'' echo, was first reported by Bloom [1] for protons in water placed in an inhomogeneous magnetic field. In that paper it was stated that the SP echo was more readily noticeable for pulse repetitions faster than the transverse irreversible relaxation time, T_2 (and hence, for that system, T_1), and was bipolar in character. It was conjectured [1] that the origin of the SP echo was due solely to strong Larmor inhomogeneous broadening (LIB), since it appeared only in inhomogeneous dc fields. However, Stearns [2], in modeling a qualitatively similar bipolar SP echo observed in ferromagnetic ^{59}Co*Co*, was unable to generate a SP echo according to the Bloom formalism when integrating over a flat spectrum of nuclear precessional frequencies. Chekmarev and co-workers [3,4] compared SP echo formation in conventional phase-modulated spin systems with frequency-modulated systems subject to large dynamical frequency shifts (DFS's) [5], and concluded that in the former the SP echo arises, fundamentally, from off-resonant effects, i.e., the radio-frequency (rf) carrier frequency is detuned from the center frequency by an amount comparable to, or greater than, the inhomogeneous linewidth. As a consequence, Kaiser [6] revisited protons in water with small LIB under off-resonant conditions, and generated SP echolike signals, in apparent support for these ideas. In parallel, Schenzle, Wong, and Brewer (SWB) [7,8] developed the theorem on coherent transients for large inhomogeneous broadening (for NMR, read LIB, analogous to inhomogeneity in the optical Bloch vector precessional frequencies), i.e., for systems where $T_2^* \sim 1/\Delta \ll T_2$, where T_2^* characterizes the transverse reversible relaxation time, and Δ is the half-width at half-maximum of the inhomogeneously broadened line. For the case of a SP excitation (repetition time much longer than T_1), SWB demonstrated that under selected excitation pulse areas SP echolike features could be observed in an oscillatory free-induction decay (OFID) of duration equal to one pulse width, thus providing an alternative explanation to Bloom's interpretation of the echolike transient in his Fig. 4. Most significantly, SWB were not directly contributing to the origin of the bipolar SP echo for faster repetition times presented in Bloom's Fig. 5, as was well appreciated by SWB [7] at the time. The quantitative correctness of the SP OFID model, extended also to essentially single-shot, two-pulse spin echoes, has been well-established for protons in water [8], assuming on-resonant pulses, no pulse distortion and sharp radio-frequency fields. Subsequently, Tsifrinovich and co-workers [9,10] demonstrated on ferromagnetic systems that deliberately induced pulse phase or amplitude distortions could enhance the magnitude of the SP echo up to six times, and concluded that its formation was not due to internal interactions within those magnetic materials (as opposed to DFS systems) but due, extrinsically, to residual pulse distortions. Interestingly, the experimental SP echoes under pulse distortion are generally unipolar in shape and therefore qualitatively different from the bipolar echoes seen in Refs. [1] and [2]. The nonintrinsic origin of the SP echo or SP echolike OFID was further promoted by Kuz'min *et al.* [11] who claimed that these effects, including multicomponent two-pulse echoes, in magnetic systems, were due to nonresonant excitation. However, in an unpublished work [12], one of us (D.K.F.) observed weak, unipolar, single-pulse echoes and secondary echoes in the elemental system ^{57}Fe*Fe*, which is an anomalously narrow-line ferromagnet for which precise on-resonance excitation conditions can be established via tuning out of nonresonant beating in the FID and echo signals. The question then arises whether the signals seen in this resonant system are due to residual parasitic pulse distortion or, alternatively, an underlying, intrinsic process is, in fact, responsible.

Aside from the DFS systems, which includes ^{59}Co*Co* at low temperatures [13], the experimental observations of the so-called SP echo can be classified into two broad categories of noninteracting spin systems: (1) those performed on protons in aqueous liquids in a deliberately imposed inhomogeneous dc field leading to significant LIB, so that $T_2^* \ll T_2 \sim T_1$ and possessing (possibly) uniform radio-frequency fields, $B_1 = \omega_1 / \gamma$, where ω_1 is the Rabi frequency in angular frequency units (note that the term Rabi frequency

is more common in optical coherent spectroscopy, describing, analogously, the strength of the laser field in angular frequency units); and (2) those performed on nuclear spins in magnetically ordered solids with invariably a significant inhomogeneity in the Rabi frequencies (leading to Rabi inhomogeneous broadening, or RIB) as well as large LIB. For example, the elemental and impurity nuclei in metallic ferromagnets are often studied under conditions of zero or near-zero applied magnetic field, while the dominant signal is generally from domain walls. Here the large RIB originates from the distribution in domain wall enhancement factors, plus a smaller distribution from the metallic skin effect. The RIB due to enhancement factor inhomogeneity for the nuclei in domain walls, together with LIB, may be considered to be dominant in our theoretical considerations for the formation of a SP echo appropriate to multidomain ferromagnets. Additional complications such as spreads of angles between rf fields and walls, domain-wall edges, and domain nuclei contributing at higher rf power, demagnetizing factor distributions on rf fields, etc., all ensure that this simplified model is most unlikely to reproduce the finer detail of experimental signals when obtained from a range of particle sizes in the traditional metallic powder specimens. However, these additional complexities involve only a matter of correctly averaging over the corresponding parameters of the fundamental equations obtained below for the magnetization vector under the nonlinear dynamics due to LIB plus RIB, and including multiple-pulse (MP) excitations.

For the second class it is common to have $T_2^* \ll T_2 < T_1$ and T_2 of order of tens to hundreds of microseconds and the temperature-dependent T_1 in the millsecond range, implying that pulse repetition rates may be readily adjusted to be fast compared with T_1, but slow compared with T_2, or, alternatively, the repetition rate may be slow compared with T_1, analogous to the SWB single-pulse domain [7,8]. The large LIB in multidomain ferromagnets is assumed primarily due to spreads in demagnetizing fields rather than impurity concentration and/or quadrupolar effects.

In this paper the nonlinear dynamics of the nuclear spins under rf pulse excitation, due to the simultaneous presence of large LIB and RIB, are followed for (i) single, distortion-free, resonant pulses and (ii) increasing pulse number in a MP train, with identical pulses repeated at intervals short compared with the longitudinal relaxation time T_1 but long compared with the transverse relaxation time T_2. The formation under solely LIB of a primary echo at Δt and weaker secondary echo signals at multiples of Δt, is unambiguously demonstrated to be the result of the cumulative effects of the MP train excitation. This echolike structure evolves from a superposition of OFID's which are extended further into the time domain than Δt because of the cumulative dephasing within each pulse of the MP train. Consequently, the primary echo at Δt is more properly described as a MP echo rather than a SP echo. The efficacy of formation of the MP echo and its associated secondary echoes with increasing pulse number is much enhanced for the case of simultaneous LIB and RIB, appropriate to multidomain ferromagnets, reflecting the more rapid dampening of the OFID with the introduction of the RIB.

Our theoretical approach using concatenation of perturbation factors (PF's) in a statistical tensor (ST) formalism is sufficiently flexible that it can follow the spin dynamics due to simultaneous double inhomogeneities (in Larmor and Rabi frequencies) appropriate to multidomain ferromagnets [2–4,9–11], incorporating pure LIB, appropriate to protons in water with a uniform rf field [1,7,8] as a simpler, limiting case. In this paper, analytical expressions are obtained for the conventional pulsed NMR signal for single (LIB) and double inhomogeneities (LIB plus RIB) under the assumption of infinite LIB for single pulses and for a MP train composed of identical pulses. These results are augmented by numerical results for finite LIB values. This ST approach, first developed to accommodate the more specialized field of γ detection of NMR on oriented nuclei [14], has recently been applied to other problems in conventional pulsed NMR [15].

The general PF formalism appropriate to rank-1 ST's and transverse geometry of experiment (GE), applicable to conventional pulsed NMR detection geometry, is introduced in Sec. II. The analysis in Sec. III is presented for the SP case with simultaneous LIB and RIB, representing the next level of complexity with respect to inhomogeneities compared to the pure LIB domain [7,8]. The results from this section demonstrate the profound influence of large RIB on modifying the well-known OFID phenomenon [7,8]. In Sec. IV the analysis is extended to the case of increasing pulse number repeated on time scales fast compared with T_1. The spin dynamics are now those due to a MP train but with the important restriction that the pulse repetition interval is long compared with T_2. At no stage is the common scenario of pulse pairs, triplets or saturation sequences on time scales short compared with T_2 considered, as this circumstance provides a very different nonlinear dynamics. Again both LIB and RIB are included from the outset and the pure LIB treated as a simpler, limiting case. In both Secs. III and IV, it is assumed that the rf pulses are distortion free. The analysis of Sec. IV shows that for both pure LIB and LIB plus RIB, it is the cumulative effects of the MP train that lead to SP echolike signal evolution and secondary echo formation. The experimental support is given in Sec. V via zero-field pulsed NMR spectra obtained from binary 2 at. % $^{51}V\!Fe$ and pure elementary (enriched) $^{57}Fe\!Fe$ ferromagnets. Section VI contains the discussion, and Sec. VII the conclusion.

II. GENERAL FORMALISM

Here the ST approach, together with the concatenation of PF's [15], is used to determine the first-rank ST's appropriate to transverse GE. It has been shown previously [15] that the magnetization vector components can be written

$$\frac{m_Y(t)}{m_0} = -\sqrt{2}\ \mathrm{Im}\{G_{1\ 1}^{0\ -1}(t)\},$$

$$\frac{m_X(t)}{m_0} = \sqrt{2}\ \mathrm{Re}\{G_{1\ 1}^{0\ -1}(t)\}, \tag{1}$$

where m_0 stands for the equilibrium value of the magnetization vector. In Eq. (1) $G_{1\ 1}^{q_1\ q_2}(t)$ is the final time-dependent PF resulting from a MP excitation. It is obtained from the concatenation of the individual PF's corresponding to the pulse excitations $\tilde{G}_{1\ 1}^{q_1\ q_2}(\Delta t_i)$ and free precession

$\overline{G_1^q{}_1^q}(\tau_i)$ over pulse durations Δt_i and inter pulse free precessions τ_i, respectively. Thus

$$G_1^0{}_1^{-1}(t)=\sum_{|q_i|\leqslant\lambda}\cdots\overline{G_1^{q_2}{}_1^{q_2}}(\tau_2)\widetilde{G}_1^{q_1}{}_1^{q_2}(\Delta t_2)\times\overline{G_1^{q_1}{}_1^{q_1}}(\tau_1)\widetilde{G}_1^0{}_1^{q_1}(\Delta t_1). \tag{2}$$

In this way the magnetization vector components can be generated in a general form for SP and MP excitations with fast or slow repetition, including complications due to strong inhomogeneous broadening, and, where necessary, irreversible relaxation. The effect of the broadening, if sufficiently large, is to significantly influence the dynamics of the spin-system during rf pulsing as well as between the pulse excitations. Corresponding expressions under pulse repetition rates low in comparison to T_1 are similar to those obtained from the solution of the Bloch equations in Refs. [1], [7], and [8] containing the most general results for SP excitations under large LIB, i.e., $T_2^*\ll T_2$.

III. SINGLE-PULSE EXCITATION (PULSE REPETITION PERIODS LONG IN COMPARISON TO T_1)

Under single-pulse excitation, the Y component of the magnetization vector obtained from Eqs. (1) and (2) which contains the RIB, is assumed, in the first instance, to be present in the sample solely due to enhancement factor inhomogeneity, can be written in the form:

$$\frac{m_Y(b,y)}{m_0}=-\frac{ax}{a^2+x^2}[1-\cos(y\sqrt{a^2+x^2})]\sin(bx)+\frac{a}{\sqrt{a^2+x^2}}\sin(y\sqrt{a^2+x^2})\cos(bx). \tag{3}$$

Here $x=\Delta\omega_j/\overline{\omega_1}$, where $\Delta\omega_j=\omega_j-\omega_0$ characterizes the Larmor frequency spread; $a=\eta/\overline{\eta}$ (or $a=\omega_1/\overline{\omega_1}$), where η and $\overline{\eta}$ are the enhancement factor (EF) and its mean value; $\omega_1=\eta\omega_1^{\rm appl}$; $\overline{\omega_1}=\overline{\eta}\omega_1^{\rm appl}$ is the mean value of the rf amplitude in angular frequency units; $\omega_1^{\rm appl}$ is the Rabi frequency of the applied rf field; $y=\overline{\omega_1}\Delta t$ is the mean value for the pulse area; Δt is the pulse duration; $b=\overline{\omega_1}\tau$ characterizes the time interval after the pulse excitation and is measured from the trailing edge of the pulse (further on, the magnetization vector component m_Y is presented as a function of b and y corresponding to the dimensionless time parameter and pulse area); and ω_0 and ω_j represent the resonance line center and the jth isochromat's precession frequency, respectively. For generality we shall first retain a in order to include both RIB and LIB. For the case of LIB only, we put $a=1$ in Eq. (3) (so then $\overline{\omega_1}=\omega_1$) and all subsequent expressions derived from Eq. (3). Before employing this expression in a numerical approach, it will be analytically examined in extreme limits by averaging over both inhomogeneities, in Larmor frequency (x) and rf amplitude (a), with their corresponding form factors. The averaging over the LIB is carried out for an inhomogeneously broadened line of assumed Gaussian form,

$$g(\Delta\omega_j)d(\Delta\omega_j)=\left(\frac{\ln 2}{\pi\Delta^2}\right)^{1/2}e^{-\ln 2(\Delta\omega_j/\Delta)^2}d(\Delta\omega_j)=\left(\frac{\ln 2}{\pi}\right)^{1/2}Re^{-\ln 2(Rx)^2}dx, \tag{4}$$

for an extremely broad linewidth, i.e., $R=\overline{\omega_1}/\Delta\to 0$, so that the form factor in Eq. (4) can be considered to be effectively constant while integrating. The integration can then be carried out using Laplace transforms [16]. For the average value of $m_Y(b,y)/m_0$ in Eq. (3), one obtains

$$\left\langle\frac{m_Y(b,y)}{m_0}\right\rangle_x=-\pi a^2 g(0)\int_b^y\left(\frac{s-b}{s+b}\right)^{1/2}J_1(a\sqrt{s^2-b^2})ds, \tag{5}$$

where $J_1(\,)$ is the Bessel function of the first order and $g(0)=\sqrt{\ln 2/\pi}R$. This expression is similar to that obtained in Refs. [7] and [8], but there $a=1$. It is important to note that, according to Eq. (5), the signal is only defined for the time interval $\tau\leqslant\Delta t$ (corresponding to $b\leqslant y$), i.e., the pulse length, which constitutes the Theorem on Coherent Transients [7]. This OFID signal is constrained as oscillations damping in time and becoming zero after a time equal to the SP duration [Fig. 1(a)], i.e., $b=\overline{\omega_1}\Delta t$.

Next, we investigate how the EF inhomogeneity, through the RIB, influences the signal. Averaging Eq. (5) over values of EF, $a=\eta/\overline{\eta}$, which are distributed with an exponential form factor [17]

$$P(\eta)d\eta=\frac{1}{\overline{\eta}}\exp\left(-\frac{\eta}{\overline{\eta}}\right)d\eta=\exp(-a)da, \tag{6}$$

and including the reverse enhancement of the signal gives the averaged value for the magnetization vector Y component

$$\left\langle\frac{m_Y(b,y)}{m_0}\right\rangle_{x,a}=\int_0^\infty\eta P(\eta)\left\langle\frac{m_Y(b,y)}{m_0}\right\rangle_x d\eta=\overline{\eta}\int_0^\infty ae^{-a}\left\langle\frac{m_Y(b,y)}{m_0}\right\rangle_x da. \tag{7}$$

As a result, according to Eqs. (5) and (7), we obtain an integral of the form [18]

$$\int_0^\infty a^3e^{-a}J_1(a\beta)da=\Gamma(5)(1+\beta^2)^{-2}P_3^{-1}[(1+\beta^2)^{-1/2}], \tag{8}$$

where $\beta=\sqrt{s^2-b^2}$, $P_3^{-1}(r)$ is the Legendre function, and $\Gamma(n)$ is the Γ function. Thus the signal for an extreme LIB ($R\to 0$) sample can be described by the doubly averaged expression

$$\left\langle\frac{m_Y(b,y)}{m_0}\right\rangle_{x,a}=-\pi\overline{\eta g}(0)E_3^{-1}(b,y), \tag{9}$$

where we introduce $E_m^n(b,y)$ functions to reflect the averaging over the EF contained in the parameter a:

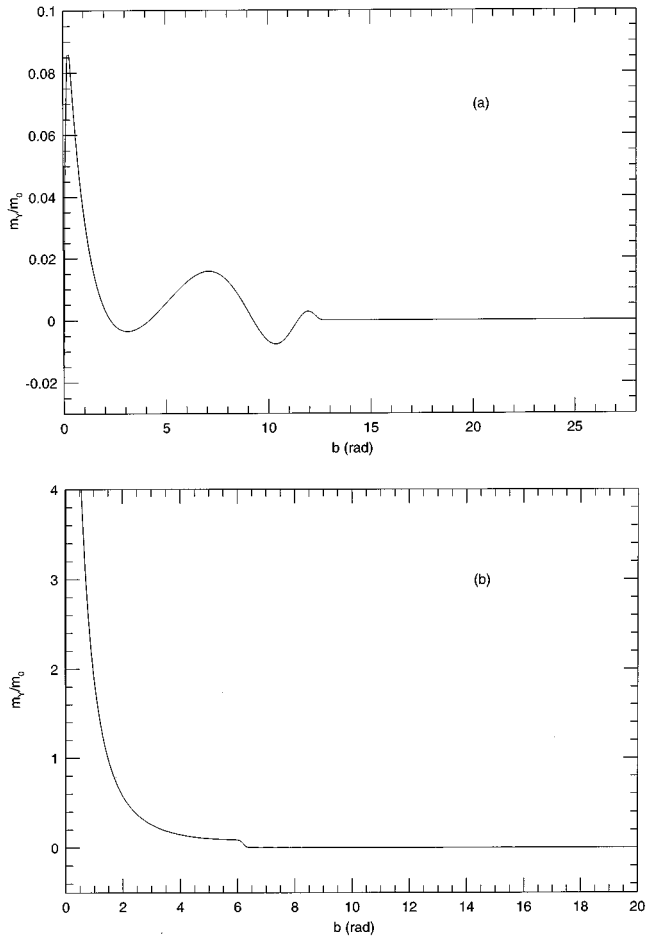

FIG. 1. (a) Oscillatory free-induction decay signal under pure LIB, using PF formalism; pulse area $y=4\pi$ and $R=\omega_1/\Delta=0.1$. (b) Step anomaly at the area (time) location of the SP echo under double inhomogeneity (LIB and RIB); $y=2\pi$ and $R=0.05$, $\overline{\eta}=100$. RIB is assumed due to the EF spread.

$$E_3^{-1}(b,y)=\Gamma(5)\int_b^y\left(\frac{s-b}{s+b}\right)^{1/2}\frac{1}{(1+s^2-b^2)^2}\times P_3^{-1}\left(\frac{1}{\sqrt{1+s^2-b^2}}\right)ds. \tag{10}$$

Here the integration over s can be carried out [18] after inserting the expression for the Legendre function $P_3^{-1}[1/(\sqrt{1+s^2-b^2})]$. After straightforward algebra, $E_3^{-1}(b,y)$ (for $b\leqslant y$) becomes

$$E_3^{-1}(b,y)=3\left\{\left(\frac{yb}{1-b^2}+1\right)R_{5/2}+\frac{1}{3}\left(\frac{4yb}{(1-b^2)^2}-\frac{yb}{(1-b^2)}-1\right)R_{3/2}+\frac{2}{3}\frac{yb}{(1-b^2)^2}\times\left(\frac{4}{1-b^2}-1\right)R_{1/2}+\frac{2}{(1-b^2)^2}-\frac{8}{3(1-b^2)^3}\right\}, \tag{11}$$

where R_ε is defined as

$$R_\varepsilon(b,y)=\frac{1}{(1+y^2-b^2)^\varepsilon}. \tag{12}$$

In analyzing Eqs. (11) and (12) the pole $b=1$ and the branch point $b=\sqrt{1+y^2}$ ($b\rightarrow\sqrt{1+y^2}$, but still $b\leqslant y$ according to the theorem of coherent transients formed under pure LIB) correspond, respectively, to the formation of anomalies near the moments of time $\tau=1/\overline{\omega_1}(b\rightarrow 1)$ and $\Delta t(b\rightarrow y)$. The latter would be traditionally associated with the formation of a SP echo, but in this case represents only the first indication of the progenitor of an echo; it was not present for the case of pure LIB. Figure 1(b) shows that the anomaly at $\tau=\Delta t(b=y=\overline{\omega_1}\Delta t)$ is better described as a step anomaly for the SP excitation, rather than an echo. This is clear since in the vicinity of $\tau=\Delta t(b=y)$ the function $E_3^{-1}(b\rightarrow y)$ starts to approach the branch point, but abruptly becomes zero when $b\geqslant y$. As we will demonstrate in Sec. IV, this step anomaly, formed under *double inhomogeneity* for a SP, rapidly evolves into the primary echo resulting from a MP train excitation. The predicted transient associated with the time $\tau=1/\overline{\omega_1}(b=1)$ is to our knowledge a new and, in some respects, more interesting effect since its position is defined by the average rf pulse Rabi frequency $\overline{\omega_1}$. We will henceforth refer to this anomaly as the ''Rabi frequency signal.'' This τ equates to a small time for multidomain ferromagnets possessing large internal rf enhancement, and this signal would generally be lost in the deadtime of the receiver. Both the ''Rabi frequency signal'' and the progenitor echo at $\tau=\Delta t(b=y)$ may be considered developments from the OFID formed under only large LIB. Figure 1(b) displays the resulting smoothly decaying signal with the initial peak, but located at $b<1$, as $R=0.05$ is different from the analytical limit $R\rightarrow 0$ corresponding to an infinitely large LIB; the effect of the $R_\varepsilon(b,y)$ terms is to cause the decay of the signal just before $\tau=\Delta t(b=y)$, and the signal terminates at the moment of time equal to the pulse duration, just as for the OFID. Thus the rf amplitude inhomogeneity (due to various physical origins, including, but not necessarily restricted to, domain-wall enhancement) if sufficiently profound ($2\pi/\overline{\omega_1}\ll\Delta t$), causes damping of the oscillations in the OFID signal and the formation of the step anomaly at $\tau=\Delta t(b=y)$. This step anomaly is not related to any external pulse distortions [9,10], as it is formed from rectangular resonant pulse excitation, nor is it a frequency modulation due to pulling resulting from a dynamic shift of the NMR frequency [5] nor nonresonant excitation [11].

IV. MULTIPLE-PULSE TRAIN (PULSE REPETITION TIMES SHORT IN COMPARISON WITH T_1)

Experimentally, SP excitation, at a high repetition rate (MP train excitation) compared with T_1, may be utilized to improve the SP echo signal [1]. The cumulative increase of a spin-echo signal, under a pure rotating but small pulse area excitation, is a well-known phenomenon [19]. But the case involving the highly nonlinear dynamics of a spin system (large LIB and, for multidomain ferromagnets in zero field, additional RIB effects) under pulse excitation is a challenging problem in the study of the formation of a spin-echo signal. Here, results from the accumulation of a signal associated with a high repetition pulse process are derived theo-

retically by increasing the pulse number from 1 to 2, then 3, 4, etc., but allowing no transverse magnetization vector components between the pulses. Thus the repetition period T satisfies the inequality $T_2^* \ll T_2 < T < T_1$, and so only the longitudinal components of the nuclear magnetization vector are of importance. As a result the dephasing of a spin system during n pulse excitations is accumulated and restored within a time interval elapsing from the trailing edge of the last $[(n+1)\text{th}]$ pulse in the MP train. It is on this basis that the evolution away from the OFID (LIB only) or the step anomaly (LIB plus RIB) shown in Figs. 1(a) and 1(b), respectively, for a SP, toward the formation of a well-defined echo at $\tau = \Delta t$, together with the emergence of secondary echoes for a MP train, is analytically and then numerically established.

Using the concatenation of PF's approach [Eq. (2)] the condition assumed for the interpulse interval T for a train of equally spaced SP's (T = const) and, more stringently, the total duration nT (neglecting, of course, relaxation within pulses) of the train of SP's plus ensuing transients, is less than T_1 but larger than T_2. Accordingly, at each successive pulse excitation of the MP train the nuclear spin dynamics starts with its axial component unchanged by longitudinal relaxation but with zero transverse components. Hence only PF's with $q=0$ are significant, prior to the last pulse, and the cumulative effects of these n pulses plus the final pulse directly lead to the formation of the time-dependent signal after the MP train. (Note that if the repetition rate is faster than T_2, i.e., $T < T_2$, then the n preceding PF's with all allowable q's have to be taken into account as in Eq. (2), and this will cause the formation of additional echo signals with location dependent on interpulse time interval. This case is not considered in this paper, and is not related to the SP echo formation. The final PF for an $(n+1)$ MP train, with each pulse of identical width Δt (and amplitude), is

$$G_{1\ 1}^{0\ -1}(t) = [\tilde{G}_{1\ 1}^{0\ 0}(\Delta t)]^n \tilde{G}_{1\ 1}^{0\ -1}(\Delta t)\ \exp\ (i\Delta\omega_j \tau). \quad (13)$$

Here τ is taken as the time interval measured from the trailing edge of the final rf pulse. n is the number of extra pulses over the original SP, previously considered in Sec. III; however, for the analysis leading to Eq. (13), and below, the MP train is better regarded as n preliminary pulses followed by the critical, final pulse which creates the transverse magnetization commensurate to the standard GE in conventional pulsed NMR. As a result, from Eq. (13), and according to Eq. (1), the transverse components of the magnetization vector are

$$\frac{m_Y(b,y)}{m_0} = \left\{ 1 - \frac{a^2}{a^2+x^2}[1-\cos(y\sqrt{a^2+x^2})] \right\}^n \times \left[-\frac{ax}{a^2+x^2}[1-\cos(y\sqrt{a^2+x^2})]\sin(bx+\phi) + \frac{a}{\sqrt{a^2+x^2}} \sin(y\sqrt{a^2+x^2})\cos(bx+\phi) \right], \quad (14a)$$

and

$$\frac{m_X(b,y)}{m_0} = \left\{ 1 - \frac{a^2}{a^2+x^2}[1-\cos(y\sqrt{a^2+x^2})] \right\}^n \times \left[\frac{ax}{a^2+x^2}[1-\cos(y\sqrt{a^2+x^2})]\cos(bx+\phi) + \frac{a}{\sqrt{a^2+x^2}} \sin(y\sqrt{a^2+x^2})\sin(bx+\phi) \right], \quad (14b)$$

where ϕ is the rf pulse phase. As before, when the rf amplitude enhancement and its associated RIB are not incorporated, we put $a=1$ in these equations. It is worth noting that the phase of the last $[(n+1)\text{th}]$ pulse is of considerable importance, appearing in both second terms, as shown explicitly in Eqs. (14a) and (14b). Further, if we assume $\phi=0$ only the Y component of the magnetization is an even function of x, and therefore it alone survives after the averaging over the LIB, although the echo phase will clearly change with different values of ϕ. Thus, should the skin effect be the major source of RIB as occurs in single-domain metallic ferromagnets, all phases are mixed so that the final magnetization vector will contain both components, in general. Further on we analyze the Y component only under strong LIB and RIB (assumed due solely to a distribution in EF's, as for multidomain ferromagnets examined under low rf power) in order to investigate the formation of secondary echoes.

The formation of SP echolike transients and the enhancement of the echo amplitude due to the cumulative excitation from the MP train can be readily demonstrated in the simplest cases $n=1$ and 2 ($n=0$ represents the SP excitation). As above, it is emphasized that n refers to those preliminary pulses in the train that are applied before the last pulse, i.e., in the PF formalism, before the relevant PF, $\tilde{G}_{1\ 1}^{0\ -1}(\Delta t)$, has been applied to create the transverse magnetization vector component.

Thus with $n=1$ in Eq. (14a), corresponding to a two-pulse sequence, the additional terms [over that in Eq. (5)] are

$$\frac{\Delta m_Y(b,2y)}{m_0} = \frac{a^3\cos(bx)}{2(a^2+x^2)^{3/2}} \sin(2y\sqrt{a^2+x^2}) + \frac{a^3 x \sin(bx)}{2(a^2+x^2)^2} \cos(2y\sqrt{a^2+x^2}), \quad (15a)$$

and

$$\frac{\Delta m_Y(b,y)}{m_0} = \frac{3a^3 x \sin(bx)}{2(a^2+x^2)^2} - \frac{2a^3 x \sin(bx)}{(a^2+x^2)^2} \cos(y\sqrt{a^2+x^2}) - \frac{a^3\cos(bx)}{(a^2+x^2)^{3/2}} \sin(y\sqrt{a^2+x^2}), \quad (15b)$$

which will cause the formation of a signal at a time equal to twice the pulse duration, or $2\Delta t (b=2y)$ [Eq. (15a)], and modify the echo signal formed at a SP duration, or $\Delta t (b=y)$ [Eq. (15b)]. After averaging over the LIB using the Laplace transform [16], for the additional terms we obtain

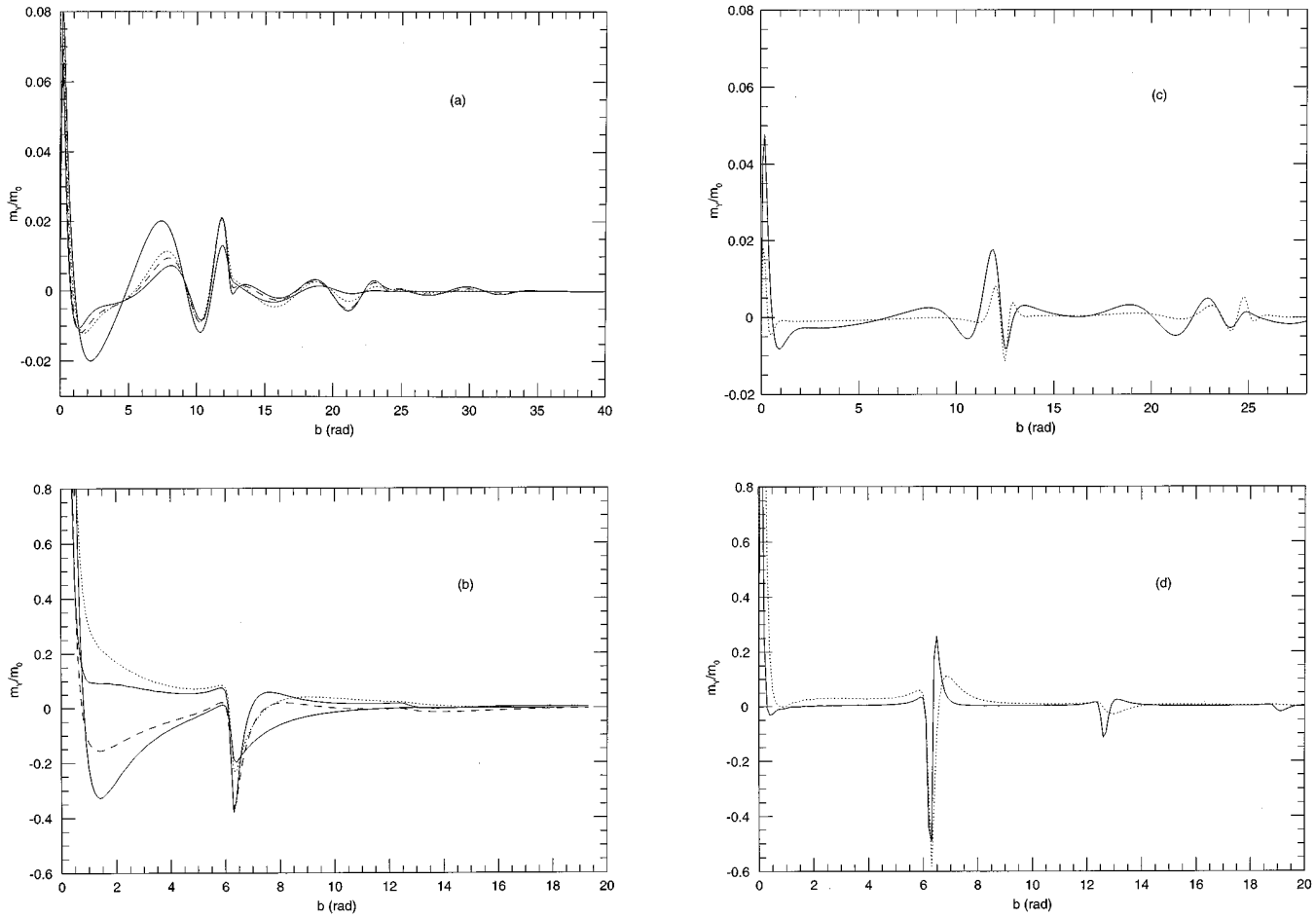

FIG. 2. (a) Initial modification away from the OFID under pure LIB for increasing pulse number with a pulse repetition rate fast compared with T_1. Preliminary pulse number $n=1$–4 (i.e., 2–5 pulses; see text), for pulse areas $y=4\pi$ and $R=0.1$. Solid line (light), $n=1$; dotted line, $n=2$; dashed line, $n=3$; solid line (heavy), $n=4$. (b) Initial evolutionary formation of the multiple-pulse echo under double inhomogeneity (LIB and RIB) for increasing pulse number with pulse repetition rate fast compared with T_1. RIB is assumed due to the EF spread. Preliminary pulse number n = 1–4 (i.e., 2–5 pulses; see text), for pulse areas $y=2\pi$, $R=0.05$, and $\overline{\eta}=100$. Solid line (light), $n=1$; dotted line, $n=2$; dashed line, $n=3$; solid line (heavy), $n=4$. Note the weak secondary echo emerging at $b=4\pi(=2y)$ for $n=4$. (c) Evolutionary formation of the multiple-pulse echo under pure LIB with a pulse repetition rate fast compared with T_1 for $n=10$ (dotted line) and 50 (solid line). $y=4\pi, R=0.1$. The formation of a secondary echo signal with increasing n can also be observed. Note the reduced abscissa span compared with (a). (d) Consolidation of the multiple-pulse echo and two secondary echoes under double inhomogeneity (LIB and RIB) with a pulse repetition rate fast compared with T_1 for $n=10$ (dotted line) and 50 (solid line). $y=2\pi$, $R=0.05$, and $\overline{\eta}=100$. RIB is assumed due to the EF spread.

$$\left\langle \frac{\Delta m_Y(b,2y)}{m_0} \right\rangle_x = \frac{\pi g(0) a^4}{4} \int_b^{2y} (2y-s)^2 \left(\frac{s-b}{s+b} \right)^{1/2} \times J_1(a\sqrt{s^2-b^2})\,ds \tag{16a}$$

and

$$\left\langle \frac{\Delta m_Y(b,y)}{m_0} \right\rangle_x = -\pi g(0) \left[a^4 \int_b^{y} (y-s)^2 \left(\frac{s-b}{s+b} \right)^{1/2} \times J_1(\sqrt{s^2-b^2})\,ds + a^3 \int_b^{y} (y-s) J_0(\sqrt{s^2-b^2})\,ds \right]. \tag{16b}$$

Note that the averaging over LIB of Eqs. (15a) and (15b) has been carried out giving the cancellation of all the terms except those given in Eqs. (16a) and (16b), and corresponding to signal with durations $b \leqslant y$ in Eq. (16b) and $b \leqslant 2y$ in Eq. 16(a). But in comparison to Eq. (5), the additional term $(2y-s)^2$ in Eq. (16a) provides an important modification to the oscillatory Bessel function. As a result the oscillatory amplitude decreases when b approaches the upper limit, which is now twice the pulse duration (note the upper limit in the integral is equal to twice the pulse area), but amplifies the oscillations when b and $2y$ (characterizing the time elapsing after the pulse train and twice the pulse width, respectively) are much different. In Eq. (16b) there is now a term $(y-s)^2$ causing similar modifications of the signal near time $\tau=\Delta t(b=y)$ and, in addition an integral of the zero-order Bessel function appears, modifying, but not extending, the duration of the oscillatory signal. Note that the total duration of the signal is now twice the pulse duration. The evolutionary changes away from the OFID for n = 1–4 can

be observed in Fig. 2(a) where pure LIB ($a=1$) is assumed. There is a systematic extension of the signal to larger areas (longer times) as n increases, and, in addition, the first indications of a concentration of an isolated signal at b equal to the pulse area (corresponding to the location of the primary echo).

After averaging over the RIB [17], assumed due to EF spread, the additional terms take the form

$$\left\langle \frac{\Delta m_Y(b,2y)}{m_0} \right\rangle_{x,a} = \pi g(0) \overline{\eta} \frac{\Gamma(7)}{4} \int_b^{2y} \frac{(2y-s)^2}{(1+s^2-b^2)^3} \left(\frac{s-b}{s+b} \right)^{1/2} P_5^{-1} \left(\frac{1}{\sqrt{1+s^2-b^2}} \right) ds \tag{16c}$$

and

$$\left\langle \frac{\Delta m_Y(b,y)}{m_0} \right\rangle_{x,a} = -\pi g(0) \overline{\eta} \left[\Gamma(7) \int_b^{y} \frac{(y-s)^2}{(1+s^2-b^2)^3} \left(\frac{s-b}{s+b} \right)^{1/2} P_5^{-1} \left(\frac{1}{\sqrt{1+s^2-b^2}} \right) ds \right.$$
$$\left. + \Gamma(5) \int_b^{y} \frac{(y-s)}{(1+s^2-b^2)^{5/2}} P_4^0 \left(\frac{1}{\sqrt{1+s^2-b^2}} \right) ds \right], \tag{16d}$$

which can be evaluated analytically as shown in Appendix A, with R_ε being slightly modified to read

$$R_\varepsilon(b,z) = \frac{1}{(1+z^2-b^2)^\varepsilon}, \tag{17}$$

with $z=y$ and $2y$. Equations (16) and (17) correspond to the signals formed at times $\tau=\Delta t$ (primary echo $b=y$) and $2\Delta t$ (first of the secondary echoes $b=2y$). There is an enhancement of the main signal formed at $\tau=\Delta t(b=y)$ due to extra terms. There remains a strong peak at $\tau=1/\overline{\omega_1}(b=1)$, the ''Rabi frequency signal,'' which is a common pole point for all terms under infinitely large LIB.

Similarly, if we put $n=2$ in Eq. (14a) it can be easily shown that an extra additional term arises in the magnetization vector component, demonstrating the formation of a secondary echo at $\tau=3\Delta t(b=3y)$:

$$\frac{\Delta m_Y(b,3y)}{m_0} = \frac{a^5 \cos(bx)}{4(a^2+x^2)^{5/2}} \sin(3y\sqrt{a^2+x^2}) + \frac{a^5 x \sin(bx)}{4(a^2+x^2)^3} \cos(3y\sqrt{a^2+x^2}). \tag{18a}$$

After averaging over LIB [note that some unimportant terms occurring after averaging of Eq. (18a) over LIB are dropped, since they cancel with the similar terms emerging when averaging of the total expression for the magnetization vector component, rather than a part of it] we obtain

$$\left\langle \frac{\Delta m_Y(b,3y)}{m_0} \right\rangle_{x} = -\frac{\pi a^6 g(0)}{4\times 4!} \int_b^{3y} (3y-s)^4 \left(\frac{s-b}{s+b} \right)^{1/2} \times J_1(a\sqrt{s^2-b^2}) ds, \tag{18b}$$

demonstrating that the total duration of the signal is now three times the pulse duration, with the higher-order dampening multiplier $(3y-s)^4$ strongly modifying the conventional Bessel function oscillations in the integral when b (and correspondingly s) approaches the upper limit of integration. At the same time when the upper limit (corresponding to triple pulse duration) and lower limits (corresponding to the time measured from the trailing edge of the final third pulse) are largely different, then this multiplier term will provide for amplification of the Bessel function oscillations. This will result in modification of the OFID signal [see Fig. 2(a)]. The other additional terms for $n=2$ are not presented here, but they will obviously accumulate into the main $\tau=\Delta t(b=y)$ echo signal, as was the case for $n=1$ and, as well, the first $\tau=2\Delta t(b=2y)$ secondary echo.

After averaging over the RIB the additional term is

$$\left\langle \frac{\Delta m_Y(b,3y)}{m_0} \right\rangle_{x,a} = -\pi g(0) \overline{\eta} \frac{\Gamma(9)}{4\times 4!} \int_b^{3y} \frac{(3y-s)^4}{(1+s^2-b^2)^4} \times \left(\frac{s-b}{s+b} \right)^{1/2} P_7^{-1} \left(\frac{1}{\sqrt{1+s^2-b^2}} \right) ds, \tag{18c}$$

which is ultimately a function of $R_\varepsilon(b,3y)$, and describes the signal formation at the triple-pulse duration. The computed curves for $n=1$–4 (corresponding to MP trains of 2–5 equal width pulses) are presented in Fig. 2(b) for double inhomogeneous broadenings. In comparison with the first case of pure LIB [Fig. 2(a)], where there is observed only a slow modification of the OFID signal for such low pulse number trains [neither the primary echo nor secondary echoes are evident in Fig. 2(a)] there is a more rapid evolution of the primary echo at $\tau=\Delta t(b=y)$ (i.e., $b=\overline{\omega_1}\Delta t$) and even for so few preliminary pulses as $n=4$ the first indications of a secondary echo at $\tau=2\Delta t(b=2y)$, begin to emerge [Fig. 2(b)].

Expression (14a) can be analyzed more generally for positive integers via use of the binomial expansion [18], in order to demonstrate the accumulated modification of the main sig-

nals and the formation of their secondary signals, both of which may be easily observed experimentally. The additional terms arising from the nuclear magnetization vector then sum from straightforward but lengthy algebra to be

$$\left\langle \frac{\Delta m_Y(b,y,2y,\ldots,ny)}{m_0} \right\rangle_x = \pi a^{2k+1} \sum_{k=1}^{n} \binom{n}{k} \Bigg\{ -aD_k^1(y) + \binom{k}{1} \left[\tfrac{1}{2} aD_k^1(2y) - aD_k^1(y) - D_k^0(y) \right] + \sum_{m=1\,(\text{if } k \geqslant 2)}^{k/2(\text{ or } (k-1)/2)} \frac{1}{2^{2m}} \binom{k}{2m}$$
$$\times \Bigg[\sum_{r=0}^{m-1} \binom{2m}{r} \left[-aD_k^1((2m-2r+1)y) - aD_k^1((2m-2r-1)y) - 2D_k^0((2m-2r-1)y) \right.$$
$$\left. + 2aD_k^1(2(m-r)y) + 2D_k^0(2(m-r)y) \right] - \binom{2m}{m} aD_k^1(y) \Bigg] + \sum_{m=1\,(\text{if } k \geqslant 3)}^{k/2-1(\text{ or } (k-1)/2)} \frac{1}{2^{2m}} \binom{k}{2m+1}$$
$$\times \Bigg[\sum_{r=0}^{m-1} \binom{2m+1}{r} \left[\tfrac{1}{2} aD_k^1(2(m-r+1)y) + \tfrac{1}{2} aD_k^1(2(m-r)y) + D_k^0(2(m-r)y) - aD_k^1((2m \right.$$
$$\left. - 2r+1)y) - D_k^0((2m-2r+1)y) \right] + \binom{2m+1}{m} \left[\tfrac{1}{2} aD_k^1(2y) - aD_k^1(y) - D_k^0(y) \right] \Bigg] \Bigg\}, \tag{19}$$

with condensed notations

$$D_k^1(z) = \frac{1}{(2k)!} \int_b^z (z-s)^{2k} \left(\frac{s-b}{s+b} \right)^{1/2} J_1(a\sqrt{s^2-b^2})\,ds, \tag{20a}$$

$$D_k^0(z) = \frac{1}{(2k-1)!} \int_b^z (z-s)^{2k-1} \left(\frac{s-b}{s+b} \right)^{1/2} J_0(a\sqrt{s^2-b^2})\,ds, \tag{20b}$$

where $z = y,\ 2y,\ \ldots,ny$.

According to Eq. (19), the final signal is a superposition of the OFID signals, and the terms corresponding to them are characterized by the duration of oscillations equal to multiples of the pulse width as follows from Eqs. (20a) and (20b) ($b \leqslant z$). In contrast to Eq. (5), they are dampened when approaching their termination time ($b \to z$), and amplified when moving away from this point ($b \ll z$); see Eq. (20a). Additional terms with zero-order Bessel functions with a similar role for the multiplier in the integral in Eq. (20b) arise, causing more profound modifications of the total signal with increasing n. As a result, for a higher pulse number in the MP train this superposition leads to dampening of the oscillations, but with localized anomalies at the moments of time which are multiples of the pulse duration, as can be observed for $n = 10$ and 50 in Fig. 2(a) for pure LIB. This clearly shows the formation of the primary echo and the first of the secondary echoes, evolved from the single pulse OFID.

When both LIB and RIB are present, and therefore requiring additional averaging over a, Eq. (19) is transformed into

$$\left\langle \frac{\Delta m_Y(b,y,2y,\ldots,ny)}{m_0} \right\rangle_{x,a} = \pi \sum_{k=1}^{n} \binom{n}{k} \Bigg\{ -E_{2k+3}^{-1}(y) + \binom{k}{1} \left[\tfrac{1}{2} E_{2k+3}^{-1}(2y) - E_{2k+3}^{-1}(y) - E_{2k+2}^{0}(y) \right] + \sum_{m=1\,(\text{if } k \geqslant 2)}^{k/2(\text{ or } (k-1)/2)} \frac{1}{2^{2m}} \binom{k}{2m}$$
$$\times \Bigg[\sum_{r=0}^{m-1} \binom{2m}{r} \left[-E_{2k+3}^{-1}((2m-2r+1)y) - E_{2k+3}^{-1}((2m-2r-1)y) - 2E_{2k+2}^{0}((2m-2r-1)y) \right.$$
$$\left. + 2E_{2k+3}^{-1}(2(m-r)y) + 2E_{2k+2}^{0}(2(m-r)y) \right] - \binom{2m}{m} E_{2k+3}^{-1}(y) \Bigg] + \sum_{m=1\,(\text{if } k \geqslant 3)}^{k/2(\text{ or } (k-1)/2)} \frac{1}{2^{2m}} \binom{k}{2m+1}$$
$$\times \Bigg[\sum_{r=0}^{m-1} \binom{2m+1}{r} \left[\tfrac{1}{2} E_{2k+3}^{-1}(2(m-r+1)y) + \tfrac{1}{2} E_{2k+3}^{-1}(2(m-r)y) + E_{2k+2}^{0}(2(m-r)y) \right.$$
$$\left. - E_{2k+3}^{-1}((2m-2r+1)y) - E_{2k+2}^{0}((2m-2r+1)y) \right] + \binom{2m+1}{m}$$
$$\times \left[\tfrac{1}{2} E_{2k+3}^{-1}(2y) - E_{2k+3}^{-1}(y) - E_{2k+2}^{0}(y) \right] \Bigg] \Bigg\}, \tag{21}$$

with condensed notations (for simplicity, b in the arguments is omitted)

$$E^{-1}_{2k+3}(z)=\frac{\Gamma(2k+5)}{(2k)!}\int_b^z\frac{(z-s)^{2k}}{(1+s^2-b^2)^{k+2}}\times\left(\frac{s-b}{s+b}\right)^{1/2}P^{-1}_{2k+3}\left(\frac{1}{\sqrt{1+s^2-b^2}}\right)ds \tag{22a}$$

and

$$E^{0}_{2k+2}(z)=\frac{\Gamma(2k+3)}{(2k-1)!}\int_b^z\frac{(z-s)^{2k-1}}{(1+s^2-b^2)^{k+3/2}}\times P^{0}_{2k+2}\left(\frac{1}{\sqrt{1+s^2-b^2}}\right)ds. \tag{22b}$$

Here $P^l_m(\ )$ are the associated Legendre functions, and $\binom{k}{p}$ are the binomial coefficients. The evaluation and analysis of the integrals in Eqs. (22a) and (22b) are presented in Appendix A, demonstrating that $E^0_{2k+2}(z)$ and $E^{-1}_{2k+3}(z)$ in Eqs. (22a) and (22b) can be, in principle, presented as a function of $R_\varepsilon(b,z)$ (with various ε) and $1/(1-b^2)$ of different orders, which is important for the formation of echo signals and the ''Rabi frequency signal,'' respectively. Hence these results show that the various upper limits for the integrals in Eqs. (21), (22a), and (22b) correspond to the formation of secondary echoes at the moments of time that are multiples of the pulse-width. The location of the last secondary echo is dependent on n. From Eq. (21) it can be seen that, for $n=1$,

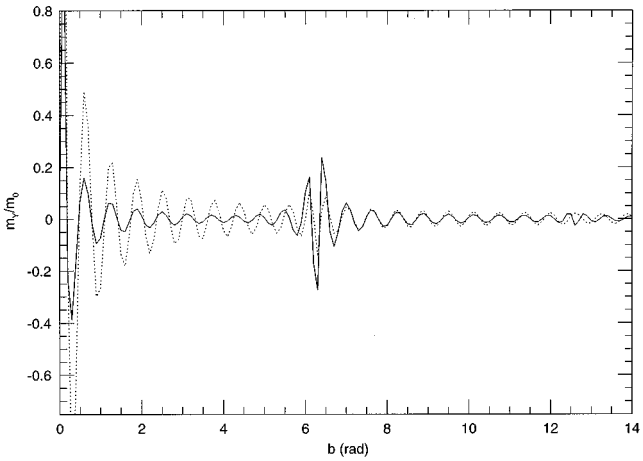

FIG. 3. Off-resonant multiple-pulse echo under double inhomogeneity (LIB and RIB) with a pulse repetition rate fast compared with T_1 for $n=10$ (dotted line) and 50 (solid line). $y=2\pi$, $R=0.05$, and $\overline{\eta}=100$. RIB is assumed due to the EF spread. The shift from the line center is equal to $10\overline{\omega_1}$.

$$\left\langle\frac{\Delta m_Y(b,y)}{m_0}\right\rangle_{x,a}=\pi[-2E^{-1}_5(y)-E^0_4(y)+0.5E^{-1}_5(2y)]; \tag{23a}$$

for $n=2$,

$$\left\langle\frac{\Delta m_Y(b,y)}{m_0}\right\rangle_{x,a}=\pi[-4E^{-1}_5(y)-\tfrac{15}{4}E^{-1}_7(y)-2E^0_4(y)-\tfrac{5}{2}E^0_6(y)+E^{-1}_5(2y)+\tfrac{3}{2}E^{-1}_7(2y)+\tfrac{1}{2}E^0_6(2y)-\tfrac{1}{4}E^{-1}_7(3y)]; \tag{23b}$$

for $n=3$,

$$\left\langle\frac{\Delta m_Y(b,y)}{m_0}\right\rangle_{x,a}=\pi[-6E^{-1}_5(y)-\tfrac{45}{4}E^{-1}_7(y)-7E^{-1}_9(y)-3E^0_4(y)-\tfrac{15}{2}E^0_6(y)-\tfrac{21}{4}E^0_8(y)+\tfrac{3}{2}E^{-1}_5(2y)+\tfrac{9}{2}E^{-1}_7(2y)+\tfrac{7}{2}E^{-1}_9(2y)+\tfrac{3}{2}E^0_6(2y)+\tfrac{7}{4}E^0_8(2y)-\tfrac{3}{4}E^{-1}_7(3y)-E^{-1}_9(3y)-\tfrac{1}{4}E^0_8(3y)+\tfrac{1}{8}E^{-1}_9(4y)]; \tag{23c}$$

and so on. From Eqs. (23a)–(23c) it is evident how the accumulation of the main signals occurs in a systematic fashion, as well as how secondary echoes form with increasing n, initially in antiphase to the previous signal for these low values of n. Due to the inherent nonlinear dynamics during the pulse excitation, the simple law of accumulation previously obtained for small rotation angles in Ref. [19] cannot be applied. But experimentally, as realized for high repetition rates compared with T_1, the secondary echoes are observed to exhibit nominally the same phase as the main echo. Numerical averaging over the double inhomogeneities for larger n ($n=10$ and 50) demonstrates [see Fig. 2(b)] the net outcome of the cumulative modifications to the primary echo and formation of secondary echo signals, now in phase with the primary echo. On the scale of Fig. 2(d) the clear emergence of a primary phase and two in-phase secondary echoes is revealed. Additional calculations (not shown) for increasing R show that the echoes are lost by $R>1$, verifying the essential need for large LIB. The computational results for finite values of R also demonstrate that the initial peak (the

''Rabi frequency signal'') has a tendency to move when R is changed, and only in the analytical limit of infinitely large LIB ($R \rightarrow 0$) is it located precisely at $b=1$.

In view of previous interest [3,6,11] in off-resonant processes as being fundamental to these transients, Eq. (14a) has been averaged over the double inhomogeneity for off-resonant excitation. For small shifts from the line center of ($\leqslant 2\overline{\omega_1}$), the changes are essentially negligible. For a stronger shift from the line center equal to $10\ \overline{\omega_1}$ (Fig. 3), calculation reveals the presence of a residual SP echolike transient among beatings of the response curve, but it is far more difficult to discern the weaker secondary echo in competition with the beating.

From our analysis, the $q=0$ dependence of the composite signal from the n preliminary pulses in the MP train will yield a stimulated echo signal whose amplitude will decrease, exhibiting T_1 dependence, when T is increased through the T_1 range toward the creation of an effective single pulse. When the extreme SP limit of $T \gg T_1$ is reached, the appropriate diagram for double inhomogeneity is Fig. 1(b), and this suggests that the secondary echoes will decrease more rapidly than the primary echo, since the secondary echoes have disappeared but the primary echo has collapsed to the step anomaly. A more detailed analysis requires the explicit introduction of perturbation factors which model the T_1 processes, which is beyond the scope of this paper.

V. EXPERIMENTAL RESULTS

Zero-field SP (strictly MP) echo signals were obtained using a coherent, B-KR321s Bruker NMR (4–200 MHz) spectrometer. Powdered samples (particle size several μm) of enriched (93.6%) $^{57}FeFe$, and ^{51}VFe (2 at.% V) were investigated at 77 K. Significant signal averaging ($2-32\times 1024$ sweeps) was necessary to characterize the features of the signals, particularly the secondary echoes. This was accomplished via the clip enhance mode on a Saicor Honeywell 43A Correlation and Probability Analyzer. Typical low to intermediate rf power, phase-sensitive detected echo signals are shown in Figs. 4–6. The detected excitation pulse, receiver deadtime, and any free-induction decay are suppressed in amplitude due to saturation of the detector.

The experimental echo is predominantly unipolar in both samples [Figs. 4(a), 5, and 6] at low rf powers, and averaging readily establishes the presence of secondary echoes at $\tau=2\Delta t$ and $3\Delta t$, for the higher pulse repetition rates. However, when the power is increased, the primary echo rapidly diminishes in amplitude, becomes bipolar, and the secondary echo is less prominent. In Fig. 4(a) (low rf power) the appearance of a secondary echo at $\tau=2\Delta t$ in-phase to the primary echo is evident for $^{57}FeFe$. Figure 4(b) shows a bipolar echo for ^{51}VFe obtained for a power level six times greater than in Figs. 5 and 6, and there is little evidence of a secondary echo. Note that the nuclear quadrupole moments for ^{51}V and ^{57}Fe are, respectively, extremely small and zero, so that quadrupolar echo effects may be ignored. As mentioned in Sec. I, the $^{57}FeFe$ sample is of particular significance because the relatively narrow linewidth (the full width at half maximum is 60 kHz) allows the on-resonance frequency to be accurately determined.

From the viewpoint of characterizing the primary echo

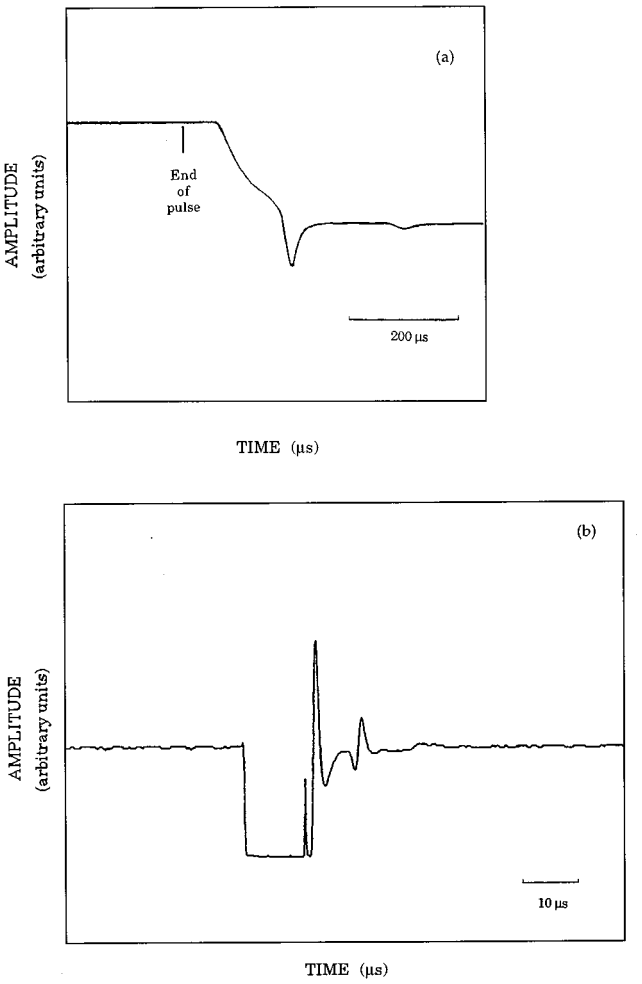

FIG. 4. (a) Low RF power multiple-pulse echoes from unambiguously on-resonant $^{57}FeFe$ showing primary and secondary unipolar echoes, in phase, at separations of one pulse width, for $T=3$ ms and $\Delta t=200\ \mu$s. $T=77$ K, $T_1=T_2=7.0(2)$ ms, $B_{\text{appl}}=0$ T, and $\omega_0/2\pi=46.54$ MHz. (b) Intermediate RF power multiple-pulse (bipolar) echo from 2 at. % ^{51}VFe at a separation of one pulse width, for $T=1$ ms and $\Delta t=10\ \mu$s. $T=77$ K, $T_1=2.0(2)$ ms, $T_2=350(50)\ \mu$s, $B_{\text{appl}}=0$ T, and $\omega_0/2\pi=97.8$ MHz.

amplitude with respect to pulse repetition rate the narrow-line $^{57}FeFe$ sample again represents a special case in the metallic ferromagnets as it was found that $T_2 \sim T_1 \sim 7$ ms (77 K), in broad agreement with the results of Ref. [20]; thus, for this sample, repetition rates fast compared with T_1 necessarily imply that they are fast compared with T_2. Such repetition rates parallel the usual case for two-pulse excitation sequences traditionally used for T_2 measurements, which, for low rf power, then lead to multicomponent spin echoes whose time location depends on the pulse pair separation as well as the pulse widths. For a MP train with $T \ll T_2$, much stronger multiple echoes, as distinct from the secondary echoes, appear, with separations tied not to the pulse width but to interpulse separation. As above, this case is not under study in the present paper. As this paper is (ideally) concerned with resonant pulses fast compared with T_1, but slow compared with T_2, a compromise pulse repetition period of 3 ms was chosen for $^{57}FeFe$. For ^{51}VFe $T_2 \sim 350(50)\ \mu$s,

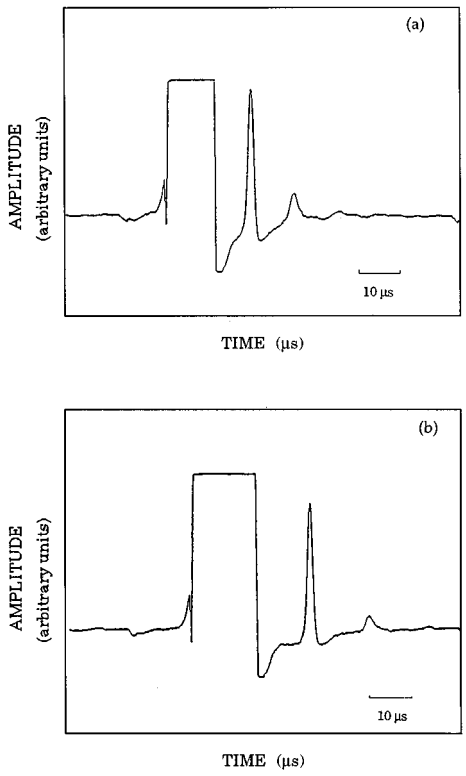

FIG. 5. Low-power multiple-pulse echoes from 2 at. % ^{51}VFe for variable pulse width (pulse area) showing primary and secondary unipolar echoes, in phase, at separations of one pulse width, for $T=1$ ms. $T=77$ K, $B_{\mathrm{appl}}=0$ T, and $\omega_0/2\pi=97.8$ MHz. (a) $\Delta t=10.5$ μs. (b) $\Delta t=14.5$ μs.

whereas $T_1\sim 2.0(2)$ ms at 77 K, so repetition periods T of 1 ms and up allow the theoretical domain of interest to be explored experimentally. The T_2 and T_1 decays were measured with a two- and three-pulse (stimulated echo) sequence, respectively, at the same low rf power, as in Figs. 4 and 5. As is usual in ferromagnets [20], the relaxation decays were nonexponential, and the errors against the relaxation times in part reflect this deviation rather than merely reflecting problems with the signal-to-noise ratio. Figure 5 shows the effect of widening pulses for a fixed amplitude for a repetition period of 1 ms, and it is observed that the primary and secondary echoes move out in the time domain occurring always at $t=\Delta t$ and $2\Delta t$. Here the pulse area between Figs. 5(a) and Fig. 5(b) has been changed sufficiently that, if this transient was merely an OFID in the SWB sense [7,8], one would expect significant variations in signal form. It is the combination of the presence of the RIB together with the high repetition rate that leads to the very strong echolike features rather than OFID features, as a function of increasing pulse width (area).

Figure 6 shows, for ^{51}VFe, a sequence of increasing pulse separation periods T, from 1 ms to 20 ms for a fixed pulse width ($\Delta t=16$ μs) and amplitude, and hence fixed pulse distortion, if present. For both samples we observe a definite reduction in the amplitude of the primary echo as the pulse repetition period increases from fast (1 ms), compared with T_1, through to slow (20 ms) compared with T_1, for a fixed pulse width, in qualitative agreement with the calculations. Figures 6(a)–6(d) also demonstrate that the secondary echo decreases more rapidly than the primary echo with increasing pulse repetition period, again a characteristic not

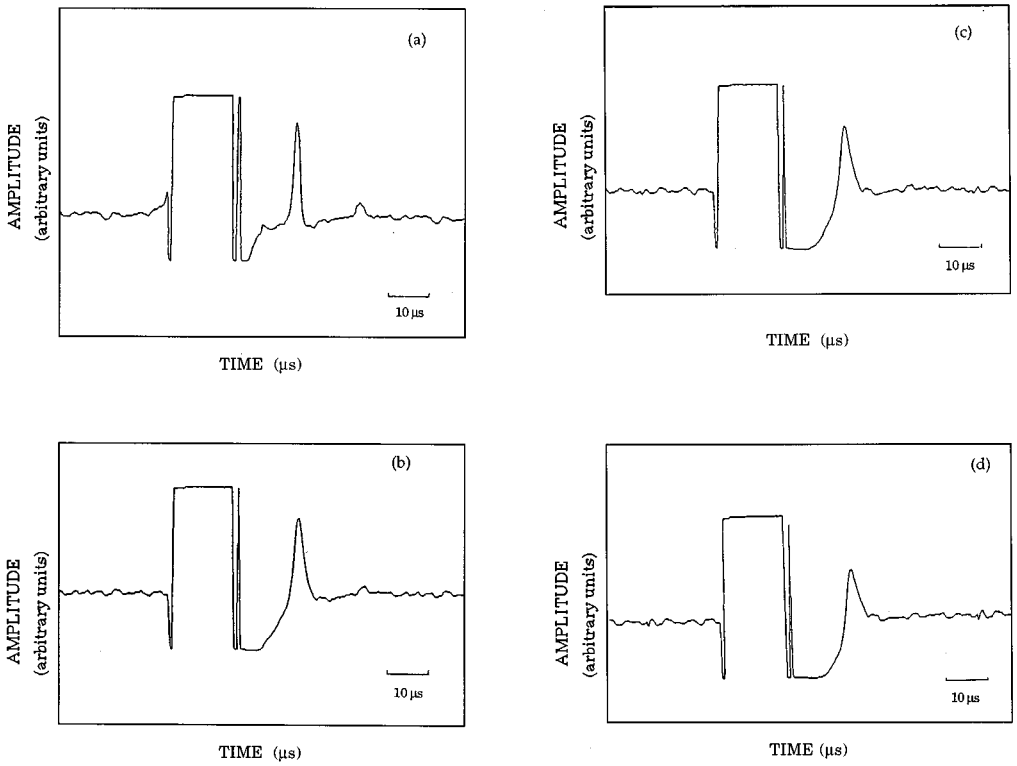

FIG. 6. Low-power multiple-pulse echoes from 2 at. % ^{51}VFe for variable repetition rate $1/T$, showing the decay in the amplitude of primary and secondary unipolar echoes at separations of one pulse width, for $\Delta t=16$ μs. $T=77$ K, $B_{\mathrm{appl}}=0$ T, and $\omega_0/2\pi=97.8$ MHz. (a) $T=1$ ms. (b) $T=5$ ms. (c) $T=10$ ms. (d) $T=20$ ms.

indicative of pulse distortion, but entirely consistent with the irreversible collapse of phase memory as nT becomes excessively long compared with T_1. As prefaced in Sec. IV, this will preferentially attenuate the secondary echoes at longest times. The fact that the amplitude of the primary echo in Fig. 6(d) is fractionally not that much smaller than in Fig. 6(a) is consistent with an observed long tail in the T_1 distribution in the ^{51}VFe sample, and/or there is some residual pulse distortion [9,10] in the spectrometer.

VI. DISCUSSION

It is shown algebraically and numerically for the case of a MP train with a pulse separation T shorter than T_1 but longer than T_2, which is in turn much longer than T_2^*, that echo formation takes place under large inhomogeneous broadening. The MP train consists of identical (equal width and amplitude), on-resonant, distortion-free pulses. The primary echo occurs at the time location typically associated with the SP echo, namely, one pulse width after the equal width excitation pulses comprising the MP train. The secondary echoes occur at multiples of the pulse width, and these effects are observed in two ferromagnets (Figs. 4–6). However, this situation is not that considered in Refs. [7] and [8] where the analysis was restricted to truly SP excitation. In the case of pure LIB this MP echo and its associated secondary echoes may be considered to be the logical extension of the theorem of coherent transients [7] for a MP train, and is, in fact, the outcome of a complicated spin dynamics representing in this special limiting case a superposition of OFID's. The superimposed OFID's total time duration is no longer restricted to one pulse width, as was central to the original theorem of coherent transients [7,8]. This constraint is fundamentally a property of dephasing only within a SP excitation. Instead, the cumulative memory of dephasing under pure LIB for $(n+1)$ pulses, occurring during the total preliminary pulse duration $(n+1)\Delta t$ of the MP train, requires correspondingly longer times to rephase in the time domain equal to $\tau=(n+1)\Delta t$. For pure LIB, the extended OFID's ultimately evolve into echoes of rapidly diminishing amplitude at multiples of the pulse width, with the strongest being at $\tau=\Delta t$. The process is much enhanced with the additional presence of RIB, as for the two ferromagnets considered here. Then the double inhomogeneous broadenings work cooperatively toward the formation of the MP echo and associated secondary echoes, in part because the RIB quickly dampens the oscillations of the OFID, as is readily seen for the case of a single pulse [Fig. 1(b)].

Our analysis suggests that the term single-pulse echo (SP echo) is a complete misnomer, as it is an OFID for SP excitation but requires a MP train for echo formation, and henceforth should be referred to as the MP echo. When $T_2^* \ll T_2 < T < T_1$ the intermediate power experimental MP echoes reproduce the theoretical curves rather well, but this may be fortuitous. It is likely that variations to the EF distribution form factor and a third integration over the skin depth will be required to obtain the essential unipolar character of MP echoes in the lower power regime. For $T_2^* \ll T < T_2, T_1$, an important second case not investigated here, it is nevertheless apparent from Eqs. (2) and (13) that the MP echo and its associated secondary echoes are formed again at times equal to multiples of the pulse width (as the $q=0$ PF's are still responsible for them). However, in addition, multicomponent echoes will also appear, determined by PF's with non-zero q's, and consequently their location will be defined by the pulse separation T and its various combinations with pulse duration. The incorporation of these nonzero PF's should not affect the MP echo formation. As for nonresonant excitation [11], our computing also demonstrates (Fig. 3) the presence of a residual MP echo, under high repetition rate under double inhomogeneity, but it is degraded from the fundamental on-resonant response, as are the secondary echoes.

VII. CONCLUSION

We conclude that the observed features of the erroneously named SP, one pulse or ''edge'' echo in NMR from multidomain ferromagnets can, in fact, be well modeled by nonlinear dynamics under a MP train excitation. The transient occurring at $\tau=\Delta t$ is therefore, fundamentally, a MP echo. Pulse distortion effects undoubtedly enhance the primary echo [9,10], and nonresonant effects may well exhibit [4,6,11] secondary echoes (still), but these extrinsic features are not essential to the MP and secondary echo formation, and are therefore considered less fundamental. Specifically, for multidomain ferromagnets, the nonlinear dynamics arise from the simultaneous presence of large LIB and large RIB. However, the profound influence of a fast pulse repetition rate with respect to the longitudinal relaxation time T_1, leading to cumulative dephasing within the pulses, is such that this class of echo, including its associated secondary echoes, may also be generated for LIB in isolation (e.g, for protons in aqueous solution in an inhomogeneous dc field, as first studied by Bloom [1], although the presence of parasitic, deliberate, or intrinsic (e.g., multidomain ferromagnets) RIB will significantly enhance the process.

ACKNOWLEDGMENTS

The authors wish to express their thanks to Dr. D. J. Isbister for initial computing support, and to Dr. S. D. James for subsequent computing support. One of us (L.N.S.) acknowledges financial support by a small ARC grant, and the hospitality of the School of Physics, University College, University of New South Wales.

APPENDIX A

The evaluation of $E^0_{2k+2}(z)$ and $E^{-1}_{2k+3}(z)$ introduced in Eqs. (22a) and (22b) can be easily carried out by use of series expansion of the corresponding Legendre functions involved within each integrand. Here we present the results as function of $(1+z^2-b^2)$ and $(1-b^2)$,

$$E^{0}_{2k+2}(b,z)=\frac{\Gamma(2k+3)}{(2k-1)!}\sum_{p=0}^{k+1}\sum_{l=0}^{k-1}\sum_{i=0}^{k-l-1}\sum_{r=0}^{l}(-1)^{p+l-r+i}\frac{(4k+4-2p)!}{2^{2k+2}p!(2k+2-p)!(2k+2-2p)!}$$
$$\times\binom{l}{r}\binom{k-l-1}{i}(1-b^2)^{l-r+i}(1+z^2-b^2)^{k-l-i-1}\left\{\binom{2k-1}{2l}zI_{2k-p-r+5/2}\right.$$
$$\left.+\binom{2k-1}{2l+1}\frac{1}{2(2k-p-r+3/2)}(R_{2k-p-r+3/2}-1)\right\} \tag{A1}$$

and

$$E^{-1}_{2k+3}(b,z)=\frac{(2k+2)!}{(2k)!}\sum_{p=0}^{k+1}(-1)^{p}\frac{(4k+6-2p)!}{2^{2k+3}p!(2k+3-p)!(2k+2-2p)!}$$
$$\times\left\{\sum_{l=0}^{k}\sum_{r=0}^{l}\sum_{i=0}^{k-l}\binom{2k}{2l}\binom{l}{r}\binom{k-l}{i}(-1)^{l-r+i}(1-b^2)^{l-r+i}(1+z^2-b^2)^{k-l-i}\right.$$
$$\times\left[\frac{1}{2(2k-r-p+5/2)}(R_{2k-r-p+5/2}-1)+bI_{2k-p-r+7/2}\right]-\sum_{l=0}^{k-1}\sum_{r=0}^{l+1}\sum_{i=0}^{k-l-1}\binom{2k}{2l+1}\binom{l+1}{r}\binom{k-l-1}{i}$$
$$\times(-1)^{l-r+i}z(1-b^2)^{l+1-r+i}(1+z^2-b^2)^{k-l-1-i}I_{2k-p-r+7/2}+\sum_{l=0}^{k-1}\sum_{r=0}^{l}\sum_{i=0}^{k-l-1}\binom{2k}{2l+1}\binom{l}{r}\binom{k-l-1}{i}$$
$$\left.\times(-1)^{l-r+i}(1-b^2)^{l-r+i}(1+z^2-b^2)^{k-l-1-i}\frac{bz}{2(2k-p-r+5/2)}(R_{2k-r-p+5/2}-1)\right\}, \tag{A2}$$

where $R_{\varepsilon}(b,z)$ (with $z=y,2y,\ldots,ny$) are defined in Eqs. (12) and (17), and $I_{n+1/2}$ are evaluated in Appendix B.

APPENDIX B

Here the evaluation of $I_{n+1/2}(z,b)\quad(n\geqslant 0)$ from Appendix A, according to [18], is presented, which is

$$I_{n+(1/2)}(b,z)=\int_{b}^{Y}\frac{ds}{(s^2+1-b^2)^{n+(1/2)}}=\frac{1}{(1-b^2)^{n}}\sum_{\nu=0}^{n-1}\sum_{\mu=0}^{\nu}\frac{(-1)^{\nu+\mu}}{2\nu+1}\binom{n-1}{\nu}\binom{\nu}{\mu}(1-b^2)^{\mu}\{zR_{\mu+(1/2)}-b\}. \tag{B1}$$

[1] A. L. Bloom, Phys. Rev. **98**, 1105 (1955).

[2] B. M. Stearns, in *Magnetism and Magnetic Materials*, edited by C. D. Graham and J. J. Rhyne, AIP Conf. Proc. No. 10 (AIP, New York, 1972), p. 1644.

[3] V. P. Chekmarev, M. I. Kurkin, and S. I. Goloshapov, Zh. Éksp. Teor. Fiz. **76**, 1675 (1979) [Sov. Phys. JETP **49**, 851 (1979)].

[4] V. P. Chekmarev and V. G. Malyshev, Fiz. Tverd. Tela (Leningrad) **30**, 1570 (1988) [Sov. Phys. Solid State **30**, 911 (1988)].

[5] Yu. Bunkov, B. S. Dumesh, and M. I. Kurkin, Pis'ma Zh. Éksp. Teor. Fiz. **19**, 216 (1974) [JETP Lett. **19**, 132 (1974)].

[6] R. Kaiser, J. Magn. Res. **42**, 103 (1981).

[7] A. Schenzle, N. C. Wong, and R. G. Brewer, Phys. Rev. A **21**, 887 (1980); **22**, 635 (1980).

[8] M. Kunitomo, T. Endo, S. Nakanishi, and T. Hashi, Phys. Rev. A **25**, 2235 (1982); M. Kunitomo and M. Kaburagi, *ibid.* **29**, 207 (1984).

[9] V. I. Tsifrinovich, E. S. Mushailov, N. V. Baksheev, A. M. Bessnertnyĭ, E. A. Glozman, V. K. Mal'tsev, O. V. Novoselov, and A. E. Reingardt, Zh. Éksp. Teor. Fiz. **88**, 1481 (1985) [Sov. Phys. JETP **61**, 886 (1985)].

[10] I. G. Kiliptari and V. I. Tsifrinovich, Sov. Phys. Phys. Met. Metalography **74**, 208 (1992); I. G. Kiliptari and V. I. Tsifrinovich, Fiz. Tverd. Tela (Leningrad) **33**, 2852 (1991) [Sov. Phys. Solid State **33**, 1611 (1991)].

[11] V. S. Kuz'min, I. Z. Rutkovskii, A. P. Saiko, A. D. Tarasevich, and G. G. Fedoruk, Zh. Éksp. Teor. Fiz. **97**, 880 (1990) [Sov. Phys. JETP **70**, 493 (1990)].

[12] D. K. Fowler, Ph. D. thesis, The University of New South Wales, 1983.

[13] G. Seewald, E. Hagn, and E. Zech, Hyperfine Interact. C **1**, 29 (1996).

[14] E. Matthias, B. O. Olsen, D. A. Shirley, J. E. Templeton, and R. M. Steffen, Phys. Rev. A **4**, 1626 (1971).

[15] L. N. Shakhmuratova, Phys. Rev. A **51**, 4733 (1995).

[16] H. Bateman, *Tables of Integral Transforms* (McGraw-Hill, New York, 1954), Vol. 1.

[17] D. K. Fowler, D. C. Creagh, R. W. N. Kinnear, and G. V. H. Wilson, Phys. Status Solidi **92**, 545 (1985).

[18] I. S. Gradshteyn and I. M. Ryzhik, *Table of Integrals, Series and Products* (Academic, New York, 1980).

[19] A. Schenzle, R. G. DeVoe, and R. G. Brewer, Phys. Rev. A **30**, 1866 (1984).

[20] M. Weger, E. L. Hahn, and A. M. Portis, J. Appl. Phys. **32**, 124S (1961).